ISSN 1063-7737, Astronomy Letters, 2015, Vol. 41, No. 10, pp. 593–600. © Pleiades Publishing, Inc., 2015.
Original Russian Text © N.M. Firstova, 2015, published in Pis'ma v Astronomicheskiĭ Zhurnal, 2015, Vol. 41, No. 10, pp. 642–650.

Connection between the Appearance of γ-Ray Sources and Hα Line Impact Linear Polarization in the July 23, 2002 Flare

N. M. Firstova*

Institute of Solar–Terrestrial Physics, Russian Academy of Sciences, Siberian Branch, P.O. Box 4026, Irkutsk, 664033 Russia

Received February 3, 2015

Abstract—During our spectropolarimetric observations of the 2B/4.8X flare on July 23, 2002, with the Large Solar Vacuum Telescope (LSVT), we detected impact linear polarization in the southern ribbon. The maximum polarization exceeded 10%. On the whole, the polarization was observed only for ~6 min out of almost 2 h of observations of this flare. At this time, the Hα line profiles had a deep central self-reversal. We have compared the LSVT observations with the Reuven Ramaty High Energy Solar Spectroscopic Imager (RHESSI) data, where the locations of γ-ray emission were obtained for the first time. A careful comparison has revealed that the effects in the Hα line were observed in a region $<10''$ located between two X-ray sources in the southern ribbon. According to the RHESSI data, a γ-ray source attributable to a beam of high-energy (~1 MeV) electrons was observed at the same place. The events in the corona and the upper chromosphere also coincide in time with the observed effects in the Hα line. The two X-ray sources are assumed to represent a common footpoint of the southern foot of the loop bifurcated due to the precipitation of high-energy electrons. It is suggested that the penetration of these electrons into the dense layers of the chromosphere could lead to impact polarization and a decrease of the Hα line intensity in the southern ribbon of the flare, in contrast to the northern ribbon where a typical hard X-ray source with an energy ~20–120 keV was observed; there were no self-reversal at the Hα line center and polarization.

DOI: 10.1134/S1063773715090029

Keywords: *Sun, polarization, particle beams.*

INTRODUCTION

At present, there are examples of successful observations of the impact linear polarization of spectral lines in solar flares (Hénoux and Semel 1981; Hénoux et al. 1983; Babin and Koval 1985; Hénoux and Chambe 1990; Firstova and Bulatov 1996; Firstova et al. 1997, 2014; Xu et al. 2005, 2006). Since the impact polarization arises under the condition of an anisotropic action on a radiating atom, these observations hypothetically allow information about the role of accelerated particle beams in heating the chromosphere during solar flares to be obtained. At the same time, according to Brown (1971), Aschwanden et al. (2002), and Fletcher (2010), the emission from the footpoints of flare loops observed in hard X rays and located in the upper chromosphere is known to be produced by the bremsstrahlung of electrons with energies 20–150 keV. Consequently, the beams of precisely such electrons put their energy into heating the chromosphere. On the other hand, low-energy electrons cannot retain their initial direction in the dense layers of the chromosphere due to Coulomb collisions. This leads to their isotropic velocity distribution; as a consequence, no polarization can arise. Vogt and Hénoux (1996, 1999) and Vogt et al. (2001) then showed that beams of low-energy protons could be a possible impact polarization mechanism. Unfortunately, there are no reliable observational data on low-energy protons. However, Emslie et al. (2000) found that at an observed energy of accelerated protons ~10 MeV, protons with energies $\leqslant$200 keV could account for a significant fraction of the total energy released during a flare. Thus, despite the fact that there is independent evidence for the bombardment of the chromosphere by the beams of energetic particles resulting from the reconnection of magnetic field lines in the corona, it is rather difficult to explain the observed polarization. Therefore, other mechanisms causing a polarization in solar flares have been proposed. For example, Hénoux and Karlický (2003) interpreted the impact polarization observed on the French–Italian THEMIS telescope in two opposite directions (radial and tangential) as evidence for the reverse current generated by the penetration of a beam of nonthermal electrons into the chromosphere during solar flares. To explain the linear polarization

*E-mail: first@iszf.irk.ru

in flares, Štěpan and Heinzel (2013) proposed resonant linear polarization due to radiation anisotropy in the inhomogeneous medium of flare ribbons.

A 4.8X flare was observed on July 23, 2002, by means of spectropolarimetry with the Large Solar Vacuum Telescope (LSVT) (Skomorovsky and Firstova 1996). Our spectropolarimetry revealed a short-lived linear polarization of a high degree. The results of our observations of this flare were preliminarily presented in Firstova et al. (2003) and in detail in Firstova et al. (2012). After a careful processing of all 250 spectrograms, polarization was detected only in 13 of them during the impulsive phase of the flare. In these spectrograms, the shape of the Hα line intensity profile in the two ribbons was different: Hα in the northern ribbon was observed completely in emission, while in the southern ribbon there was a deep self-reversal at the line center. A linear polarization of a high degree (up to 15%) was detected only in the ribbon with line self-reversal; there was no polarization in the other ribbon.

Quite a few publications ($\sim$60) are devoted to this flare. This is attributable both to certain uniqueness of the flare and to the fact that this was the first powerful flare where hard X-ray observations with a high spatial resolution were performed, and the γ-ray emission in lines and continuum was localized for the first time with the instruments onboard the Reuven Ramaty High Energy Solar Spectroscopic Imager (RHESSI). The goal of this paper was to compare the results of our LSVT observations in the chromosphere with the RHESSI data obtained for the corona and upper chromosphere in this flare.

In the first section, we briefly describe the differences in Hα line intensity and polarization between the two flare ribbons. In the second section, we show the difference between the two footpoints of the loop (or loops) based on the simultaneous RHESSI data. In the third section, we make an attempt to explain qualitatively the spectropolarimetric effects observed in this flare with the LSVT.

THE DIFFERENCES IN Hα LINE INTENSITY AND POLARIZATION BETWEEN THE TWO FLARE RIBBONS

Spectropolarimetric observations of the flare were carried out with the LSVT, which has a theoretical spatial resolution of 0.3″ and a spectral resolution of the spectrograph in the working orders of $\sim$0.01 Å. A rhombohedron separating the ordinary and extraordinary rays and allowing the solar spectrum to be simultaneously recorded in two mutually orthogonal polarizations was installed behind the spectrograph slit. The spectra were recorded with a Princeton Instruments CCD camera (512 × 512). In each spectrogram, one pixel corresponds to 0.17″ and 0.0197 Å. During the observations, the most interesting (often just the brighter ones) flare regions were placed on the spectrograph slit. The flare began at $\sim$00:18 UT in the active region NOAA 0039 at S13E72. The maximum of the Hα, microwave, and HXR (RHESSI) emission occurred at $\sim$00:28–00:31 UT; the maximum in soft X rays (GOES) occurred later, at 00:35 UT. Figure 1 presents the results taken from Lin et al. (2003), where the development in time of the fluxes from this flare in hard X-ray and γ rays obtained on RHESSI and in soft X rays on GOES is shown. The vertical lines in Fig. 1 separate the flare into three phases: the initial, impulsive, and gradual ones. The LSVT observations were carried out from 00:32:09 UT to 02:19 UT. In the observations during the impulsive phase (when polarization was detected), no $\lambda/2$ plate was used, i.e., only the Stokes parameter Q was determined. Despite the fact that we observed the entire flare for almost 2 h, evidence for polarization was obtained only during the impulsive phase.

Even during the impulsive phase, polarization was not detected in all spectrograms. The monitoring was performed visually through an interference–polarization filter (IPF) with a passband at the Hα line center installed in the light reflected from the spectrograph slit. In the first minutes of observations, there was an image of two flare ribbons with long emission wings on the CCD camera monitor screen, while the slit in the IPF eyepiece was seen to cross only one flare ribbon. This is because the Hα line center in one of the ribbons was in absorption. However, the observer tried to set both flare ribbons visible in the IPF, i.e., in the Hα line core, on the spectrograph slit, which caused the number of polarization detections to decrease.

Evidence for a linear polarization was found only in the part of the southern ribbon where the Hα line profile had a strong central self-reversal, i.e., in the part of the flare that was not visible in the emission. The difference in Hα line intensity profiles in the two flare ribbons is shown in Fig. 2. One of the two orthogonal, simultaneously obtained stripes of the spectrum for different times of the impulsive phase are presented here. The hard X-ray RHESSI image of the flare superimposed on the BBSO Hα line image is also given.

It can be seen from Fig. 2 that in hard X rays, one footpoint of the flare loop is located on the northern ribbon and two footpoints are located on the southern one. We think that the northern foot of the loop rests on the bright emission ribbon of the flare, while there is no emission under the two HXR sources in part of the southern foot of the loop, at least at the Hα line center. If we turn to the spectrograms in Fig. 2,

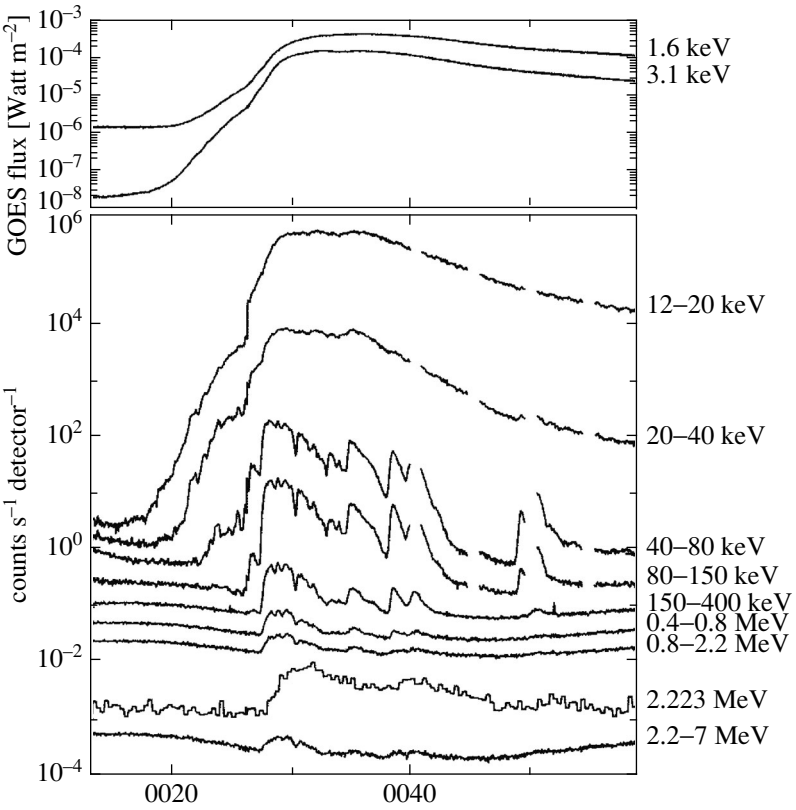

Fig. 1. Development of the X-ray and γ-ray emission in various energy bands during the development of the July 23, 2002 flare (Lin et al. 2003).

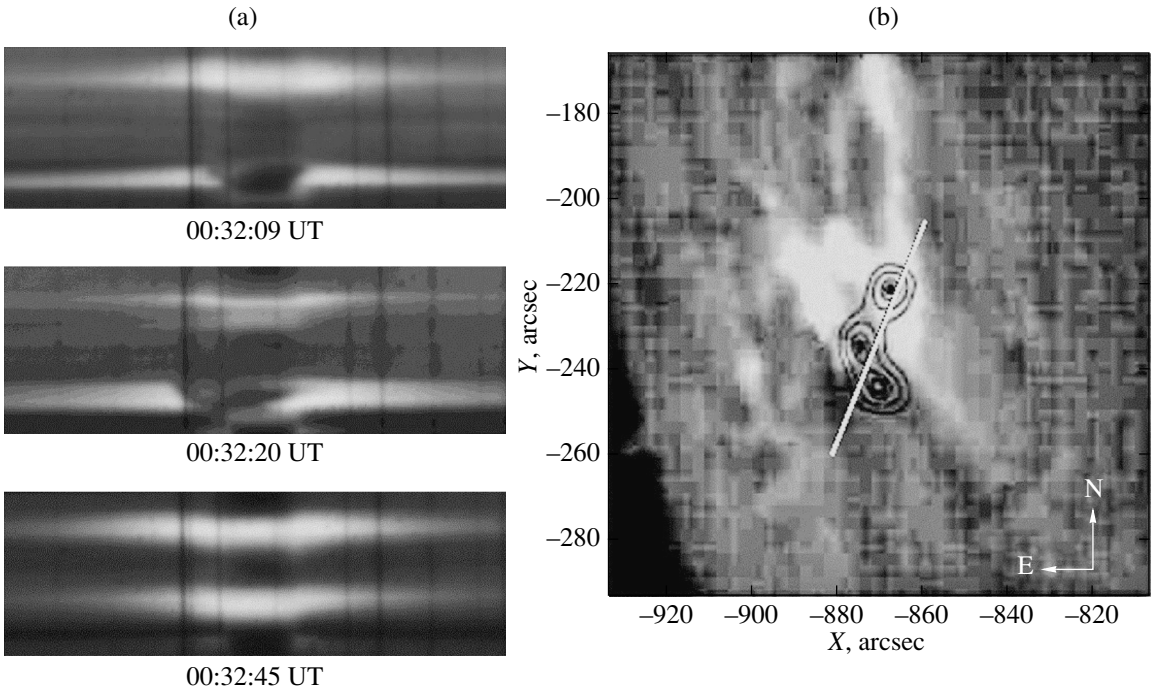

Fig. 2. (a) The spectrograms (for one of the two orthogonal stripes of the spectrum) obtained with the LSVT during the impulsive phase. (b) The hard X-ray (RHESSI) image of the flare superimposed on the BBSO Hα image. The white line indicates the position of the LSVT spectrograph slit during the impulsive phase.

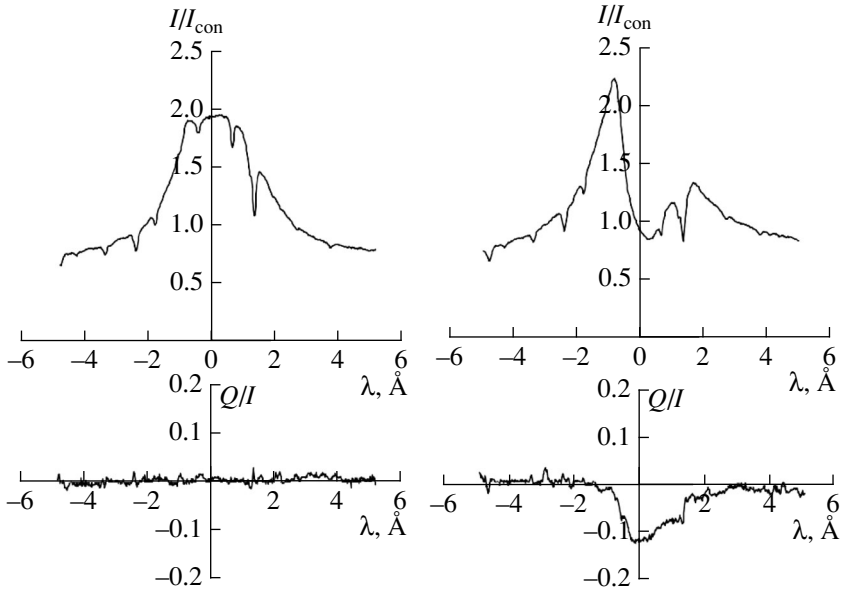

Fig. 3. Top: an example of the Hα line intensity profiles averaged over two stripes of the spectrum in the two flare ribbons (with and without self-reversal). Bottom: the profiles of the Stokes parameter Q/I obtained using these intensities.

then it can be seen that in the southern ribbon there is no emission only in the line core, while the wings reflecting deeper chromospheric layers are in emission. In the first two spectrograms, the distance between the flare ribbons is $\sim 20''$. Once the spectrograph slit has been moved to the region of the ribbons with emission at the line center, the distance between the ribbons was $\sim 13''$. According to Lin et al. (2003), the distance between the loop footpoints in hard X rays is $\sim 13''$.

Over the period of our LSVT spectropolarimetric observations of the impulsive phase of the July 23, 2002 flare from 00:32:09 UT (the beginning of our observations) to 00:44:36 UT, we took 57 spectrograms. In each spectrogram, we made 10–12 cuts along the dispersion with a step across the flare ribbon of $0.51''$ or $0.85''$ (3 or 5 pixels).

Evidence for a linear polarization was found only in 13 spectrograms. In the remaining cases, the Stokes parameters did not exceed the measurement errors. Basically, the polarization was 2–6%, and occupied $2''$–$4''$. In three spectrograms where maximum polarization (greater than 10%) was observed, the size of these regions was $\sim 6''$. In all cases of the existence of polarization, a deep self-reversal was observed at the Hα line center. All these results refer only to the southern flare ribbon. Figure 3 shows examples of two profiles of the Hα line intensity and Stokes parameters with zero and negative values. It can be seen that there is no polarization when the Hα line profile is a purely emission one, without any absorption at the line center.

THE DIFFERENCE IN HARD X-RAY EMISSION AT THE LOOP FOOTPOINTS OF THE JULY 23, 2002 FLARE

The RHESSI data allow one to see the hard X-ray sources with a high spatial resolution and to localize the γ-ray sources. At least three hard X-ray sources (with an energy above 30 keV) observed during the impulsive phase could be identified with the footpoints of coronal magnetic loops. Figure 4 presents the positions of all X-ray sources in this flare taken from Emslie et al. (2003): the coronal source (soft X rays) and the X-ray sources at the loop footpoints in various energy bands.

We will designate the northern HXR source as $f1$ (Krucker et al., 2003). The southern ribbon will then be located under HXRsources $f2$ and $f3$ according to Fig. 2.

Observers of flares with an Hα filter have long noticed the divergence of flare ribbons. The standard magnetic reconnection models predict an increase in the separation of the footpoints during the development of a flare, which probably occurs due to the motion of the boundaries of the footpoint HXR sources as a result of the subsequent reconnections of magnetic field lines.

Krucker et al. (2003) presented the motion of the X-ray sources not perpendicular to but along the ribbons, essentially parallel to the neutral line along the ribbon. In the northern ribbon of this arcade, source $f1$ moved with a systematic velocity up to ~ 50 km s^{-1} along the ribbon for more than 10 min. The superhot coronal source (with an energy

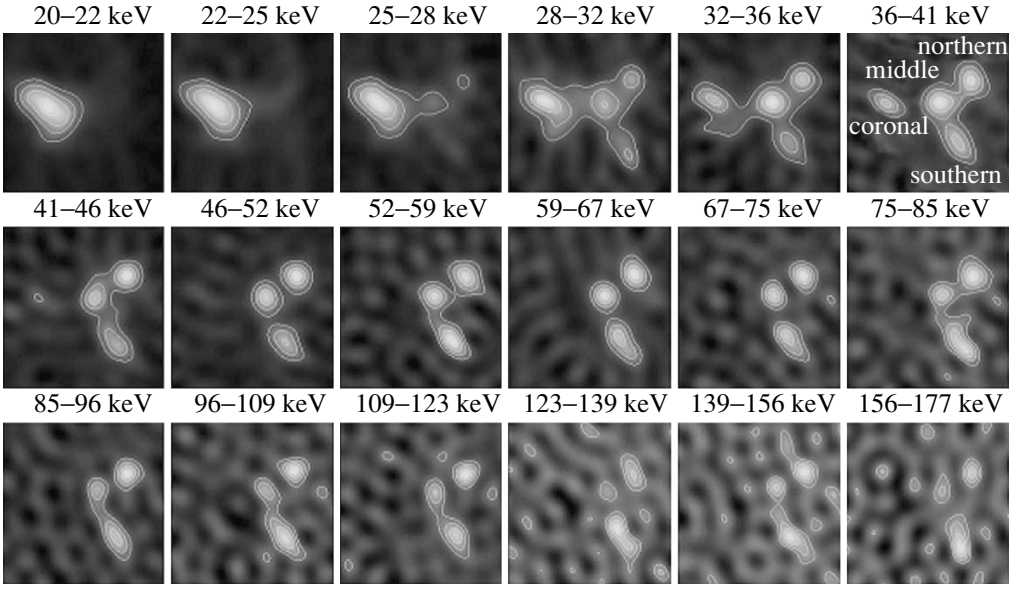

Fig. 4. Positions of the X-ray sources in various energy bands in the time interval ~00:28–00:30 UT. The designations of these sources are given in the image with an energy 36–41 keV.

$\leqslant$30 keV) moved with a comparable velocity in the same direction as the northern source ($f1$). The continuous motion along a straight line suggests that the footpoints of the earlier loops in the northern ribbon lie near the later loop. The two sources $f2$ and $f3$ in the southern ribbon moved in the same direction, but the systematic motion lasted no more than half a minute with the dominance of different sources ($f2$ or $f3$) at different times.

Our version of the unusual motion of sources $f2$ and $f3$ is as follows: these sources are one common footpoint of the southern foot of the loop, while their separation into two is caused by the penetration of a beam of high-energy electrons into this loop. This led both to an increased total size of these sources and to a less systematic motion along the ribbon. Figure 5 taken from Hurford et al. (2003) presents a more complete picture of the penetration of nonthermal particles into the chromosphere during the impulsive phase of the flare. According to this figure, γ-ray sources also produced by the bremsstrahlung of electrons with a higher and even relativistic energy are located between $f2$ and $f3$ (hard X-ray sources with an energy 30–100 keV). The maximum size of these sources is ~7.5″ (Fig. 5).

Using this flare as an example, Lin et al. (2003) and Hurford et al. (2003) showed for the first time that the beams of relativistic electrons and electrons with an energy of tens of keV are located in the same place. In addition, it follows from Fig. 1 that the high-energy electrons penetrated into the chromosphere at the same time as the high-energy ions, but the positions of the latter are offset by $20'' \pm 6''$ from the place of electron precipitation (Fig. 5). Emslie et al. (2004) believe that the precipitation of ions is associated with the presence of large-scale loops.

Additional evidence that sources $f2$ and $f3$ are one common loop footpoint is the fact that at 00:32:30 UT (Fig. 6) source $f3$ ceased to exist (Krucker et al. 2003), i.e., approximately when the beam of high-energy electrons disappeared at ~00:32 UT (Fig. 1). Furthermore, Fig. 6 shows a good correlation of the time dependence of all sources, suggesting that they have a common reconnection process.

We considered the behavior of the hard X-ray sources at the footpoints of the arcade of flare loops reflecting the penetration of electron beams with an energy 30–100 keV into the chromosphere and responsible for the excitation of hydrogen atoms and the formation of flare ribbons in the chromosphere. The northern emission ribbon in the Hα line and the northern X-ray source $f1$ can be attributed to a typical representation of the development of a flare in the thick-target model (see, e.g., Fletcher, 2010). However, the formation of a deep self-reversal at the Hα line center and the appearance of a linear polarization in a small region of the southern foot of the ribbon ($<10''$) may be associated with the penetration of streams of high-energy electrons with an 300–1400 keV into the chromosphere.

THE INFLUENCE OF BEAMS OF HIGH-ENERGY ELECTRONS ON THE Hα LINE

We associate the observed differences in the behavior of the Hα line in the two flare ribbons

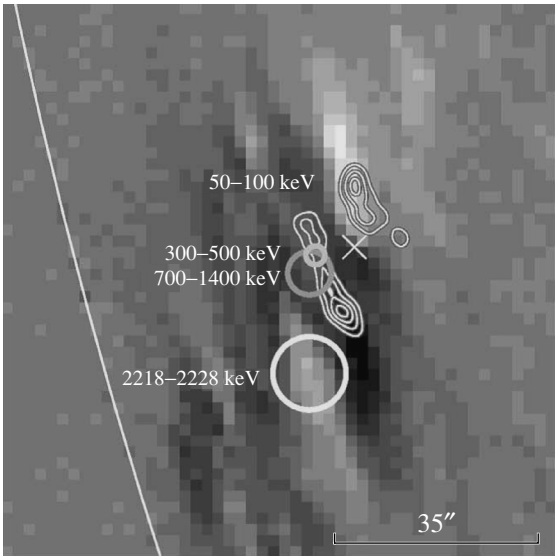

Fig. 5. Positions of the X-ray and γ-ray sources (Hurford et al. 2003). The isophotes indicate the hard X-ray sources; the gray circles indicate the γ-ray emission in the 300–500 and 700–1400 keV energy bands attributable to the precipitation of high-energy electrons; the white circles indicates the γ-ray emission in the 2218–2228 keV line caused by ions.

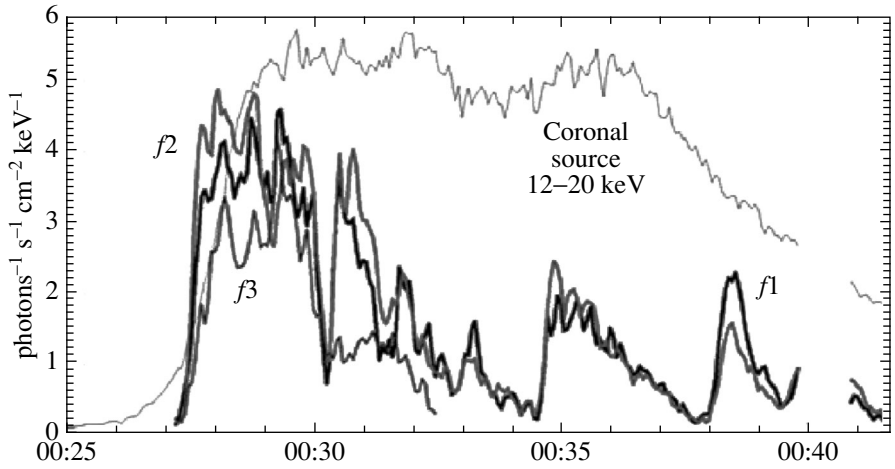

Fig. 6. Time dependence of three X-ray sources at the impulsive phase of the flare (Krucker et al. 2003).

with the difference in bremsstrahlung at the loop footpoints caused by an additional beam of high-energy electrons in the southern foot of the flare. As can be seen from Fig. 2, the place of intersection of the spectrograph slit with the southern ribbon lies at the boundary between $f2$ and $f3$, i.e., coincides with the γ-ray emission source produced by the bremsstrahlung of high-energy and relativistic electrons. The main γ-ray burst began at ~00:28 UT and ended at ~00:33 UT; three small bursts lasted until ~00:41 UT (Fig. 1). The spectrograms in which the highest polarization and the deepest self-reversal of the Hα line were detected were obtained at 00:32:09, 00:32:09, and 00:38:13 UT. After 00:44:36 UT, no case of impact linear polarization was detected. Thus, the effects we observed in the southern ribbon coincide with the γ-ray emission produced by the bremsstrahlung of high-energy electrons not only in space but also in time.

According to Fang et al. (1993) and Kasparova and Heinzel (2002), the central self-reversal of the Hα line under the action of nonthermal electrons during a flare depends on the increase in particle flux and, insignificantly, on the decrease in power-law index δ, i.e., the increase in electron energy. However, the maximum electron energy was usually taken to be ~100–150 keV in the calculations, as follows from the hard X-ray observations of the loop footpoints. The inclusion of a fraction of high-energy particles was not considered.

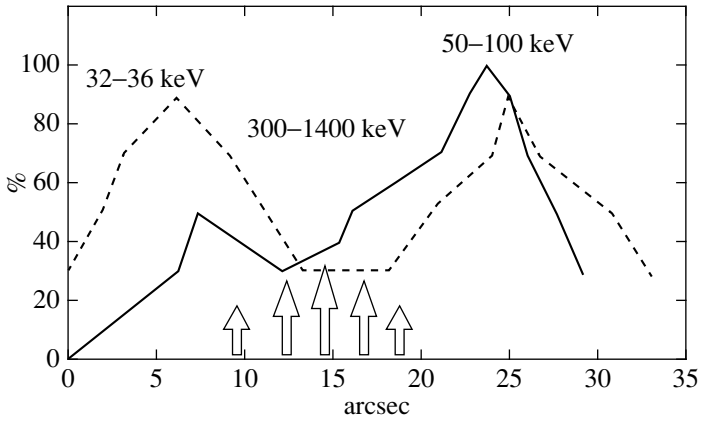

Fig. 7. Sketch showing the distribution of electrons with different energies in the beam directed toward the southern ribbon. The solid and dashed lines were constructed from the isophotes in the 50–100 and 32–36 keV energy bands, respectively. The arrows indicate the positions of high-energy electrons.

Figure 7 presents a sketch showing an approximate cross-sectional size of the beam along the southern ribbon for two energy bands. This size was obtained from the isophotes in Figs. 4 and 5 in the 50–100 (solid line) and 32–36 keV (dashed line) bands. It can be seen from Fig. 4 that the distribution of the hard X-ray intensity in different bands from 28 keV to 123 keV is similar: a dip between $f2$ and $f3$ is seen everywhere. The arrows in Fig. 7 indicate the location of the beam of high-energy electrons. In the region of high-energy electron penetration ($<10''$, where the effects in the Hα line were observed), the number of photons of other energies decreased by an order of magnitude. Consequently, in the southern foot of the loop, a redistribution of the electron energy compared to the northern foot through an increase in the fraction of high-energy particles must occur. Despite the fact that the beam of high-energy electrons is very small, they can cause a deep self-reversal for various reasons. First, these particles can increase the ionization; thus, the opacity for the Hα line emission in the upper chromospheric layers will increase. Second, more energetic electrons penetrate into deeper chromospheric layers, and, as Heinzel (2003) pointed out, if the Hα line core is formed above the region of maximum energy introduced by electrons, a brightening will appear mainly in the line wings. Thus, the deep central self-reversal of Hα in the southern ribbon may stem from the fact that high-velocity electrons pass directly into the middle layers of the chromosphere, bypassing its more rarefied upper part.

High-energy electrons can also lead to impact polarization of the Hα line, because such electrons should not be scattered in the chromosphere. Their velocity distribution function will then not lose its anisotropy, which can lead to impact polarization. If we take $\mu = \cos\upsilon$, where υ is the deviation of the angle of electron motion from its initial direction μ_0 as it collides with a hydrogen atom, then, according to Emslie (1978), μ/μ_0 depends on the electron energy E_i. If, according to Vogt and Hénoux (1999), we take the Coulomb logarithms Δ, Δ', and Δ'' to be 10, the column density in the Hα formation layer to be 1.8×10^{20} cm^{-2}, and μ_0 to be one, then for μ/μ_0 we can write

$$\frac{\mu}{\mu_0} \approx \left(1 - 10^{-35}\frac{1.8 \times 10^{20}}{E_i^2}\right)^{1/3}. \qquad (1)$$

Then, starting from an energy of 150 keV, the ratio μ/μ_0 will be equal to one. Thus, a decrease in the fraction of low-energy electrons in the southern branch of the loop and an increase in the fraction of high-energy electrons, which do not change their initial direction when entering the chromosphere, can give rise to impact polarization.

CONCLUSIONS

Owing to the image of the location of γ-ray emission in various energy bands obtained for the first time on RHESSI and the high spatial resolution of the LSVT, it turned out to be possible to compare in space and time the events occurred in the corona and upper chromosphere, on the one hand, and in the layer of the chromosphere where the line Hα is formed, on the other hand, during the July 23, 2002 flare. The precipitation of high-energy electrons took place only in a small part of the southern flare ribbon ($<10''$). According to the LSVT spectropolarimetric observations, impact polarization and a deep self-reversal at the Hα line center were detected at the same place, while in the other part of the ribbon and in the entire northern ribbon these phenomena were not detected.

The events in the corona and upper chromosphere also coincide in time with the observed effects in the Hα line. The main γ-ray burst caused by the bremsstrahlung of high-energy electrons lasted from ~00:28 UT to ~00:33 UT; three small bursts lasted until ~00:41 UT. The spectrograms in which the highest polarization and the deepest self-reversal of the Hα line were detected were obtained at 00:32:09, 00:32:09, and 00:38:13 UT. We surmise that the penetration of high-energy electrons could lead to impact polarization and a deep self-reversal of the Hα line in the southern flare ribbon.

ACKNOWLEDGMENTS

This work was performed within the framework of the "Geoeffective Processes in the Solar Chromosphere and Corona" Program of the Siberian Branch of the Russian Academy of Sciences II.16.1.5, State registration number 01201281651.

REFERENCES

1. M. J. Aschwanden, J. C. Brown, and E. P. Kontar, Solar Phys. **210**, 373 (2002).
2. A. N. Babin and A. N. Koval, Solar Phys. **98**, 159 (1985).
3. J. C. Brown, Solar Phys. **18**, 489 (1971).
4. A. G. Emslie, Astrophys. J. **224**, 241 (1978).
5. A. G. Emslie, J. A. Miller, E. Vogt, J.-C. Henoux, and S. Sahal-Brechot, Astrophys. J. **542**, 513 (2000).
6. A. G. Emslie, E. P. Kontar, S. Krucker, and R. Lin, Astrophys. J. **595**, L107 (2003).
7. A. G. Emslie, J. A. Miller, and J. C. Brown, Astrophys. J. **602**, L69 (2004).
8. C. Fang, J. C. Henoux, and W. Q. Gan, Astron. Astrophys. **274**, 917 (1993).
9. N. M. Firstova and A. V. Boulatov, Solar Phys. **164**, 361 (1996).
10. N. M. Firstova, J.-C. Henoux, S. A. Kazantsev, and A. V. Bulatov, Solar Phys. **171**, 123 (1997).
11. N. M. Firstova, V. I. Polyakov, and A. V. Firstova, Solar Phys. **279**, 453 (2012).
12. N. M. Firstova, V. I. Polyakov, and A. V. Firstova, Astron. Lett. **40**, 449 (2014).
13. N. M. Firstova, Z. Xu, and C. Fang, Astrophys. J. **595**, L131 (2003).
14. L. Fletcher, Mem. Soc. Astron. It. **81**, 616 (2010).
15. P. Heinzel, Adv. Space Res. **32**, 1293 (2003).
16. J.-C. Henoux and G. Chambe, J. Quant. Spectrosc. Rad. Transfer **44**, 193 (1990).
17. J.-C. Henoux and M. Karlicky, Astron. Astrophys. **407**, 1103 (2003).
18. J.-C. Henoux and M. Semel, in *Proceedings of the International Conference on the Year of Solar Maximum, Simferopol, 1981,* Vol. 1, p. 207.
19. J.-C. Henoux, G. Heristehi, G. Chambe, B. Woodgate, R. Shine, J. Beckers, and M. Machado, Astron. Astrophys. **119**, 233 (1983).
20. G. J. Hurford, R. A. Schwartz, S. Krucker, R. Lin, D. M. Smith, and N. Vilmer, Astrophys. J. **595**, L77 (2003).
21. J. Kasparova and P. Heinzel, Astron. Astrophys. **382**, 688 (2002).
22. S. Krucker, G. J. Hurford, and P. Lin, Astrophys. J. **595**, L103 (2003).
23. R. Lin, S. Krucker, G. J. Hurford, D. M. Smith, H. S. Hudson, G. D. Holman, R. A. Schwartz, B. R. Dennis, G. H. Share, R. J. Murphy, A. G. Emslie, C. Johns-Krull, and N. Vilmer, Astrophys. J. **595**, L69 (2003).
24. V. I. Skomorovsky and N. M. Firstova, Solar Phys. **163**, 209 (1996).
25. J. Štmpan and P. Heinzel, Astrophys. J. **778**, L6 (2013).
26. E. Vogt and J.-C. Henoux, Solar Phys. **164**, 345 (1996).
27. E. Vogt and J.-C. Henoux, Astron. Astrophys. **349**, 283 (1999).
28. E. Vogt, S. Sahal-Brechot, and V. Bommier, Astron. Astrophys. **374**, 1127 (2001).
29. Z. Xu, J.-C. Henoux, G. Chambe, M. Karlicky, and C. Fang, Astrophys. J. **631**, 618 (2005).
30. Z. Xu, J.-C. Henoux, G. Chambe, A. G. Petrashen, and C. Fang, Astrophys. J. **650**, 1193 (2006).

Translated by G. Rudnitskii